



ELECTRIC VEHICLE PROPELLED BY DUAL-INDUCTION MOTORS STRUCTURE: EXPERIMENTAL RESULTS

DJAMEL BENOUDJIT^{1,2}, SAIDD RID², NASREDDINE NAIT-SAID², MOHAMED SAIDNAIT-SAID^{2,3}, LARBI CHRIFI-ALAOUI⁴

Keywords: Electric vehicle (EV); Electric differential; Induction motor; Propulsion structure; Vector control.

An electric vehicle (EV) is an adaptation of a conventional vehicle with the integration of electrical motors. It is one of the most promising technologies that can significantly improve vehicle performance and polluting emissions. The drive association's many EV configurations and possibilities can be envisaged according to EV performances, weight, and cost. This paper presents the experimental validation of an electric differential speed action resulting from the proposed structure of an electric vehicle using dual-induction motors vector controlled, placed at the rear wheels operating at a different speed. This controls the vehicle speed of the left and right wheels during steering maneuvers. For this purpose, to perform this experimental validation and prove the main functionalities of the proposed structure, a test bench was implemented containing an actual laboratory motor placed in the left rear wheel and a motor simulation model for the right one. The outcomes show that the experimental results confirm the validity and usefulness of the proposed propulsion structure.

1. INTRODUCTION

Due to their beneficial effects on environmental protection and energy conservation, electric vehicle (EV) technologies are becoming mature and more attractive for road transportation, particularly in urban areas [1–3]. The development of electric vehicles has been encouraged and promoted by many international institutions and governments in many global projects, showing the evident recognition of the importance of energy use and global environmental problems.

EVs are similar to conventional vehicles, which are already optimized for minimum energy consumption in rolling at low speed and aerodynamics at high speed. EV is an adaptation of conventional vehicles with electromechanical systems (electrical motors) integration. In these systems, the electric propulsion structure or power train is the central part of the electric vehicle. It is in the energy transformation chain between the batteries and the rolling parts. The electric propulsion structure is to interface the electric supply with vehicle wheels, transferring energy in either direction as required, with high efficiency, under the driver's control at all times.

Moreover, for EVs, the weight reduction of the heavy different parts is mandatory due to the direct impact on electric energy consumption, which seriously affects vehicle autonomy. Therefore, the major challenges are a limited driving range and high cost [1]. Other research works on advanced EV configurations and drive association possibilities have been proposed and developed in the literature, depending on the propulsion structure type, the motor type, and efficient motor control techniques to extend the driving range and reduce the cost.

The choice of EV configuration mainly depends on the size and application of electric vehicles; the major criteria for selection are compactness, performance, weight, and cost [3]. For EV propulsion, the system configuration can be single or multiple motors, *e.g.*, one to four electrical motors, direct current or alternating current motors, with or without a clutch and a gearbox, *etc.* [2–8].

The multiple-motor configuration uses dual or four motors to independently drive individual wheels (*e.g.*, an in-wheel motor or all-wheel drive arrangement) [9–16].

One advantageous and interesting solution uses a dual-motor configuration in which two electric motors separately

drive the vehicle's rear wheels via fixed gearing (reduction of the motor speed to the desired wheel speed and high substantial torque) [3]. This configuration provides the propulsion forces through motors inside the driving wheels without requiring any mechanical component. While the two motors operating at different speeds are independently controlled, the differential action can be electrically achieved. So, the vehicle structure is simplified, and its operations and efficiency can be improved, thus increasing the vehicle range, which is an essential factor for EVs.

The overall performance of an EV depends largely on the motor type and its control strategy. An electric motor is much better suited to propel a vehicle than a combustion engine. Electric vehicles could, therefore, have better efficiency during energy conversion and produce no carbon dioxide emissions associated with the combustion process with lower noise. In addition, an electric motor offers high torque at a lower speed. It can recover energy when slowing down; the motor becomes a generator and provides energy to the batteries.

This paper deals with the experimental results of a propulsion structure that may be used in EV substituting the conventional mechanical differential system, using dual-induction motors vector controlled, which drives the vehicle's rear wheels separately. This one controls the vehicle speed of the left and right wheels during steering maneuvers. Each of these dual-motor is a standard three-phase squirrel cage induction motor. According to [17–19], induction motor drives are best suited for electric vehicle propulsion due to their low cost, high reliability, high speed, established converter, and manufacturing technology [20].

Experimental results are carried out to validate the performances of the structure via a test bench platform based on dual-induction motors vector control. For this purpose, the main idea consists of using a real laboratory induction motor placed in the left rear wheel and a mathematical motor (simulation model) for the right one.

The paper is organized as follows. Section 2 presents the field-oriented control of an induction motor intended for an electric propulsion structure. The proposed dual-induction motors structure will be presented in section 3.

In section 4, we will first illustrate the main idea of the proposed experimental platform. Then, experimental results will demonstrate the proposed structure's feasibility and effectiveness. Finally, some conclusions are given.

¹Health and Safety Institute, University of Batna 2, 53 Constantine Street, 05078, Fesdis, Batna, Algeria, d.benoudjit@univ-batna2.dz

²LSP-IE'2000 Laboratory, Electrical Engineering department, University of Batna 2, Algeria, saiddrid@ieec.org, n.naitsaid@univ-batna2.dz

³Higher National School of Renewable Energies, Environment & Sustainable Development, Batna, Algeria, m.naitsaid@hns-re2sd.dz

⁴Innovative Technologies Laboratory, University of Picardy Jules Verne, 02880 Cuffies, France, larbi.alaoui@u-picardie.fr

2. VECTOR CONTROLLED INDUCTION MOTOR

Field-oriented control (FOC) is a strategy that provides torque control of an induction motor (IM) as a separately excited dc motor by decoupling the torque and flux [21]. According to the strategy used to establish the flux position, FOC can be defined as direct or indirect field-oriented control. The last is the simplest method to overcome the difficulty of acquiring the flux rotor value in direct field-oriented control without mounting any sensors. Rotor flux is estimated (without any flux sensor) according to the measured stator currents and speed.

The main expressions used for indirect field-oriented control of an IM are as follows [22–26]:

The orientation rotor flux constraints are expressed by:

$$\phi_{rq} = 0 \text{ and } \phi_{rd} = \phi_r. \quad (1)$$

ϕ_{rq}, ϕ_{rd} denote quadrature, direct rotor flux components.

Consequently, once the above rotor flux orientation assumptions are verified, the stator voltage equations can be written as follows:

$$\begin{cases} v_{sd} = (R_s i_{sd} + \sigma L_s \frac{di_{sd}}{dt}) + e_q, \\ v_{sq} = (R_s i_{sq} + \sigma L_s \frac{di_{sq}}{dt}) + e_d. \end{cases} \quad (2)$$

e_q, e_d denote the nonlinear coupling terms

$$\begin{cases} e_d = \omega_s (\sigma L_s i_{sd} + \frac{M}{L_r} \phi_r), \\ e_q = \frac{M}{L_r} \frac{d\phi_r}{dt} - \sigma L_s \omega_s, \end{cases} \quad (3)$$

R_s, L_s denote stator winding resistance and inductance; σ is the redefined leakage inductance; i_{sd}, i_{sq} , denote direct, quadrature stator current components; ω_s, M, L_r , and ϕ_r are, respectively, the synchronous angular speed, mutual inductance, rotor inductance, and rotor flux.

The rotor flux formulation after orientation is given by:

$$\phi_r = \frac{M}{1+T_r s} i_{sd}. \quad (4)$$

T_r denotes rotor time constant, $s = \frac{d}{dt}$ Laplace operator.

This means that under rotor field-oriented conditions, the rotor flux is linearly controlled from the stator direct current component i_{sd} , using a first-order transfer function with a time constant T_r .

The rotor flux orientation is achieved by its position angle as follows:

$$\Theta_s = \int \left(\frac{M i_{sq}}{T_r \phi_r} + p \Omega \right) dt \quad (5)$$

The electromagnetic torque is expressed by:

$$T_e = p \frac{M}{L_r} \phi_r i_{sq}. \quad (6)$$

p denotes the number of pole pairs, Ω the mechanical speed.

From eq.(6) the electromagnetic torque can be controlled only from quadrature stator current component i_{sq} when the rotor flux is maintained constant. This is appropriate for EV applications, for which the loads can vary broadly. From this point of view, the induction motor does not operate normally in the field weakening region, thus, the flux must be maintained constant to its rated value. The PI controllers help control the stator current components and used for the speed

control and their parameters are determined by the pole placement method.

3. ELECTRIC PROPULSION STRUCTURE

For a conventional vehicle, when a turn is reached, the differential speed of the rear wheels is regulated by a mechanical differential to avoid vehicle slipping. So, when the inner wheel speed is reduced, the outer one is increased [9]. Besides the mechanical means, the differential action of an EV when cornering can be electrically provided by two electric motors operating at different speeds [10].

In this work, in order to show the connection with prior published studies [26–30], we use the same electric propulsion structure purpose for an EV (Fig. 1), for which the speed difference is regulated by an electric differential based on two induction motors operating at different speeds, driving separately the rear wheels of the vehicle via fixed gearing.

The differential function must verify the following expressions [26–30]:

$$\begin{cases} \Omega_{left} = \Omega_o + \Omega_{diff} \\ \Omega_{right} = \Omega_o - \Omega_{diff} \end{cases} \quad (9)$$

where $\Omega_{left}, \Omega_{right}$ are the speeds of left motor and right motor; Ω_o, Ω_{diff} is the EV speed and differential speed.

From the above equations of system (9), the vehicle speed Ω_o and the difference speed Ω_{diff} may be done simply by [26–30]:

$$\begin{cases} \Omega_o = \frac{1}{2} (\Omega_{left} + \Omega_{right}), \\ \Omega_{diff} = \frac{1}{2} (\Omega_{left} - \Omega_{right}). \end{cases} \quad (10)$$

In this structure, for each motor, the electric energy is transferred via a bi-directional power electronic converter (pulse width modulated inverter: PWM Inverter), which is controlled through the simplest strategy: indirect field-oriented control (controller bloc: FOC motor).

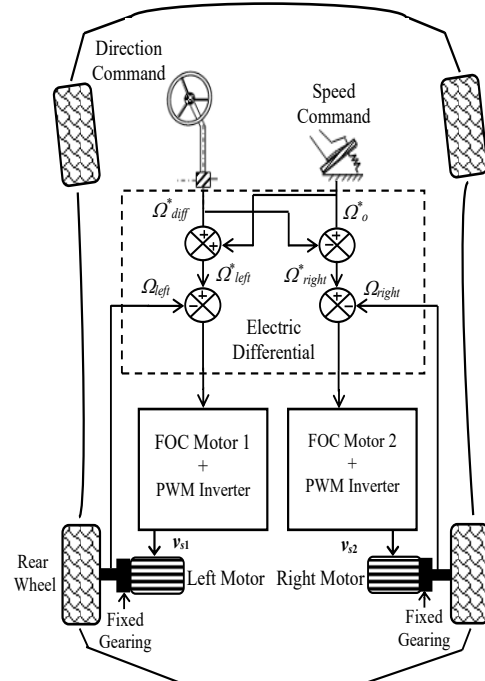


Fig. 1 –Electric propulsion structure [26–30].

Further, in previously published papers, for example, in reference [26], we used the same EV propulsion structure with robust speed control application using Fractional-Order Controller. In [27], always with the same structure, we used another application: system failures (such as an offset fault in the speed sensor and a zero-feedback sensor speed fault). In [29], the principal application is the incipient short circuit fault impact on the service continuity of an electric vehicle propelled by a dual induction motors structure. Finally, [30] highlights, always via simulation results, the impact of the emulation of load torque acting on one of both electric motors placed at the rear wheels of the EV structure during drive cycle operation and unpredictable load profiles. Compared to prior published papers, where the “propulsion structure” remains the same in terms of theoretical concept, the novelty of this work lies in the experimental implementation of this propulsion structure, which incorporates a particular combination of a real laboratory motor and its corresponding mathematical model.

4. EXPERIMENTAL VALIDATION AND DISCUSSION

Experimental validation of the electric differential principle resulting from the proposed propulsion structure was performed on a test bench to demonstrate its efficiency. For this purpose, Fig. 2 illustrates a synoptic scheme of the experimental test bench. The main idea consists of using a dual-induction motor, containing an actual laboratory motor placed in the left rear wheel and a mathematical induction motor (simulation) model for the right one. The real and simulated models have the same rated data parameters given next in Table 1 (Appendix). The described experimental test bench has been performed to test the effectiveness and the validity of the electric differential principle resulting from the proposed structure, mainly when the vehicle accomplishes the turning maneuvers.

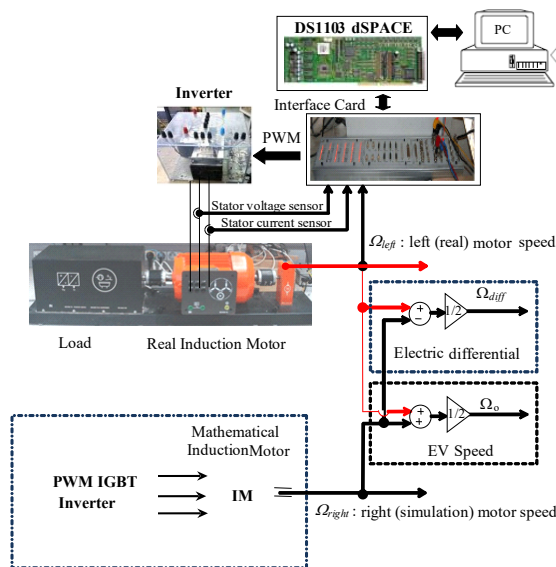


Fig. 2 – Synoptic scheme of the experimental test bench.

The test bench hardware consists of a voltage-fed IGBT inverter, a DSpace DS1103 research and development LEM-v, LEM-I sensors to perform measurements on the stator controller board, a three-phase network supply, voltage,

stator phase currents, and two motors: one a real laboratory squirrel cage induction motor of rated power 0.9 kW and a mathematical induction motor (simulation) model.

Let us first take a given speed profile, as illustrated in Fig. 3, by a speed reference trajectory where the vehicle starts with constant acceleration until it attains the reference speed of $140 \text{ rad}\cdot\text{s}^{-1}$. After there, the vehicle makes a turn toward the right; it follows that the outer (left) wheel will rotate faster than the inner (right) wheel: $\Omega_{left} > \Omega_{right}$. Then the vehicle should directly continue its trajectory at a constant cruising speed, which equals the two motors' speeds: $\Omega_{right} = \Omega_{left}$. After this, the vehicle will turn again to the left, resulting in an increase of the right motor speed compared to the left one: $\Omega_{left} < \Omega_{right}$. Finally, the vehicle directly continues its trajectory. As illustrated in Fig. 3, the speed reference trajectory is tracked more by the left (real) and the right (simulation) motors.

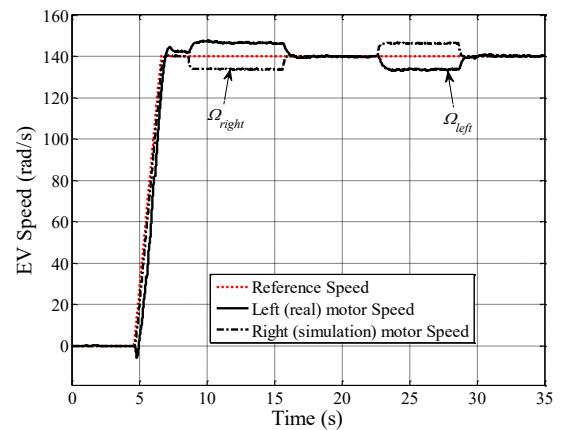


Fig. 3 – Speed versus time.

Figure 4 illustrates the differential speed commands (rectangular pulse) which constitute the reference profiles required to satisfy the above-imposed trajectory for the EV structure. Despite a disturbing oscillation at the starting acceleration, the differential speed reacts very well to a direct order given by the reference Ω_{diff}^* . Figures 5 and 6 show the evolution of stator current components for the real motor. Figures 5 and 6 depict the effectiveness of decoupling the variables-based vector control. So, flux and torque can be separately controlled, similar in performance to a dc separately excited motor control.

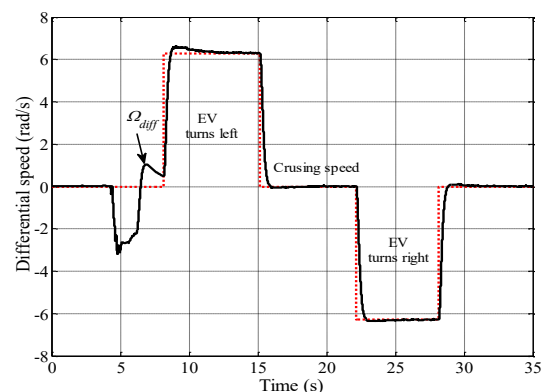


Fig. 4 – Differential speed versus time.

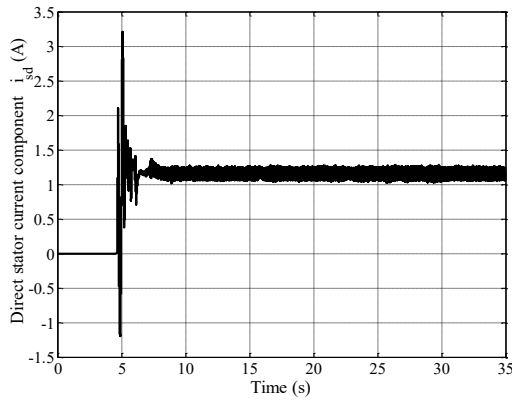


Fig. 5 – Direct current component *versus* time.

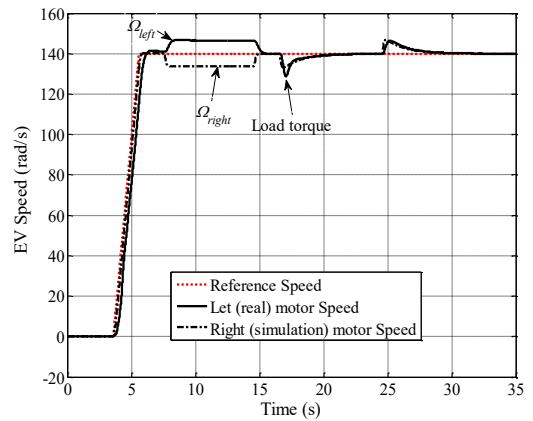


Fig. 8 – Speed *versus* time.

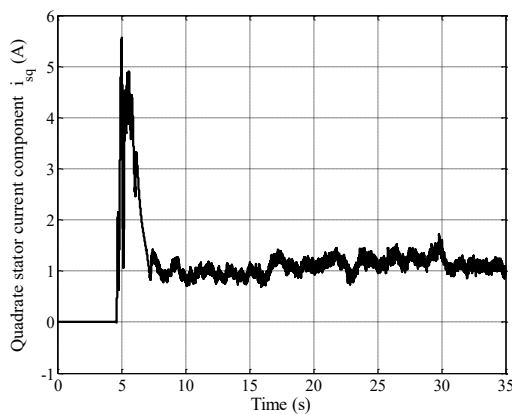


Fig. 6 – Quadrate current component *versus* time.

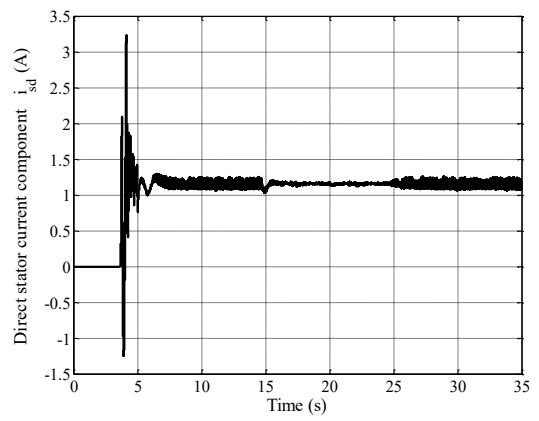


Fig. 9 – Direct current component *versus* time.

Figure 7 shows the time evolution of the first phase stator current specifically for the real motor. The current behaves according to the dynamic behavior of the motors. Figures 8 to 15 present the above responses but in presence of load, perturbation was applied at 17 s and removed at 24 s. In these tests, the vehicle starts with constant acceleration until attains the reference speed of $140 \text{ rad}\cdot\text{s}^{-1}$. After there, the vehicle makes a turn towards the right and then the vehicle should directly continue its trajectory at a constant cruising speed. As can be seen in Fig. 8, the control system reacts very well to the load perturbation and the speed response follows its reference.

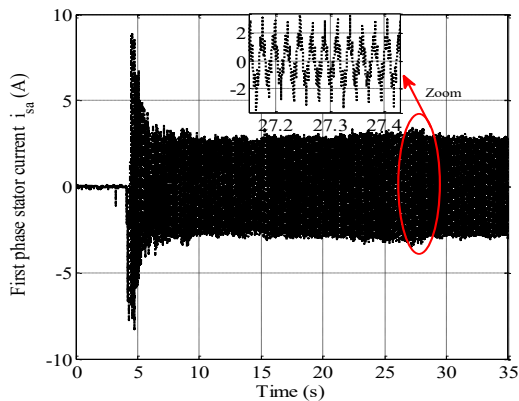


Fig. 7 – Stator current *versus* time.

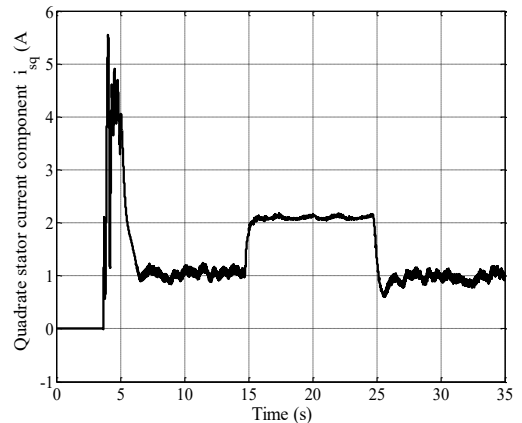
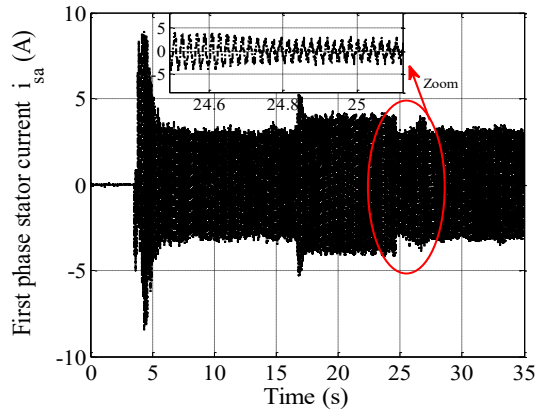
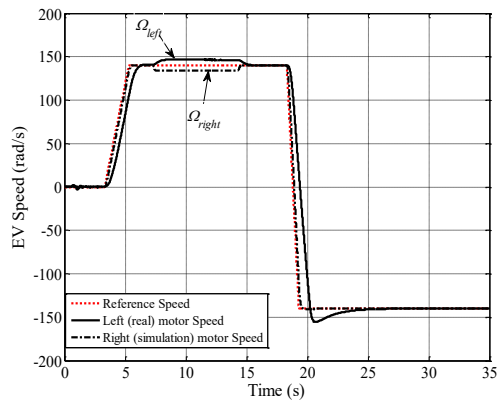
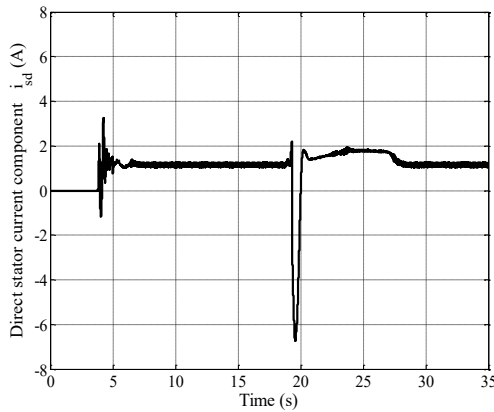
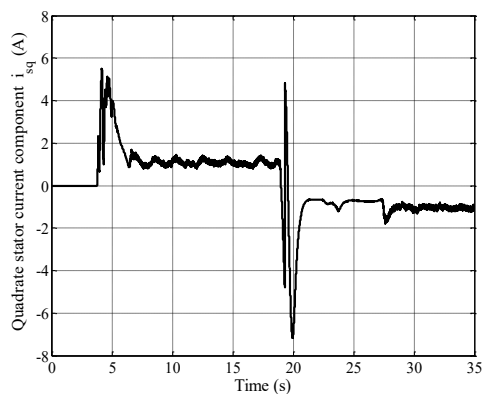


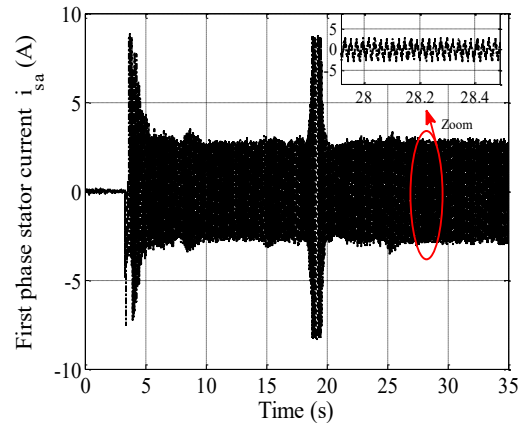
Fig. 10 – Quadrate current component *versus* time.

Despite load perturbation, Figs. 9 and 10 show that the decoupling between the current components inside the real motor required in field oriented control is quite maintained. Fig. 11 illustrates the stator current evolution for the real motor, depending in this case, on the load torque change, where its magnitude changes following the developed load torque.

Further, another test is carried out to test severely the proposed structure performances, as shown further in Figs. 12 to 15, always with the same profile but with the inversion speed for the real motor.

Fig. 11 – Stator current *versus* time.Fig. 12 – Speed *versus* time.Fig. 13 – Direct current component *versus* time.Fig. 14 – Quadrature current component *versus* time.

Figures 13 and 14 show the effect of speed inversion on the currents responses components according to the d- and q-axis. Finally, Fig. 15 presents the effect of the inversion speed on the line stator current (authorized limits).

Fig. 15 – Stator current *versus* time.

5. CONCLUSION

The main goal of this research work was to validate via a test bench platform the electric differential principle resulting from the proposed propulsion structure may be used in EV substituting the conventional mechanical differential system, using dual-induction motors vector controlled which drive separately the rear wheels of the vehicle, particularly when the vehicle accomplishes the turning maneuvers. For this purpose, the main idea consists of using a laboratory motor placed in the left rear wheel and a mathematical induction motor (simulation) model for the right one, which is the identification of a laboratory motor.

The experimental results verify that the proposed control structure operates correctly regarding speed tracking and load torque rejection.

Further its highlights the importance of continued research and analysis on this topic, as it demonstrates the need to explore multiple perspectives and approaches with other applications to better understand and validate the feasibility and effectiveness of the proposed propulsion structure. In fact, these performances via experimental results, confirm the propulsion structure validity and usefulness for an interesting application in the EV domain.

Ultimately, the goal is to identify the most effective and efficient control for the given structure application, so that the best possible results can be achieved.

Received on 10 October 2022

APPENDIX

Table 1
Induction motor parameters

Parameters	Values
Power	0.9 kW
Speed	1400 rpm
Stator resistance R_s	12.72 Ω
Rotor resistance R_r	05.15 Ω
Stator inductance L_s	0.4491H
Rotor inductance L_r	0.4331 H
Mutual inductance M	0.4331 H
Rotor inertia J	0.0035 kg \cdot m ²
Number of pole pairs p	2

REFERENCES

1. C.C. Chan, *The state of the art of electric, hybrid and fuel cell vehicles*, Proc. of the IEEE, **95**, 4, pp. 704–718, (2007).
2. P. Wheeler, T. S. Sirimanna, S. Bozhko, K. S. Haran, *Electric/Hybrid-Electric aircraft propulsion systems*, Proc. of the IEEE, **109**, 6, pp. 1115–1127, (June 2021).
3. C.C. Chan, *The state of the art of electric and hybrid vehicles*, Proc. of the IEEE, **90**, 2, pp. 247–275, (Feb. 2002).
4. S. J. Rind, Y. Hu, J. Wang, L. Jiang, *Configurations and control of traction motors for electric vehicles: A review*, Chinese Journal of electrical engineering, **3**, 3, pp. 1–17, (Dec. 2017).
5. A. Anto, M. V. Sreethumol, *Review of electric vehicles*, International Conf. on control, power, communication, and computing technologies (ICCPCTT), Kannur, India, pp. 392–398 (23-24 Mar. 2018).
6. L. Braun, M. Armbruster, F. Gauterin, *Trends in vehicle electric system design: State-of-the art summary*, IEEE vehicle powerand propulsion conference (VPPC), Canada (19-22 Oct. 2015).
7. R. Pietracho, L. Kasprzyk, D. Burzyński, *Electrical propulsion systems in vehicles—an overview of solutions*, Proc. of the International Conf. applications of electromagnetics in modern engineering and medicine (PTZE), Poland, pp. 130–133 (09-12 June 2019).
8. I. Alcalá, A. Claudio, G.V. Guerrero, *Analysis of propulsion systems in electric vehicles*, 2nd International Conf. on electrical and electronics engineering (ICEEE), Mexico, pp. 309–313 (Sep. 2005).
9. E. Mehrdad, V. S. Krishna, O. B. Hari, T. M. Ramin, *State of the art and trends in electric and hybrid electric vehicles*, Proc. of the IEEE, **109**, 6, pp. 967–984 (2021).
10. C.C. Chan, A. Bouscayrol, K. Chen, *Electric, hybrid, and fuel-cell vehicles: Architectures and Modeling*, IEEE Trans. on vehicular technology, **59**, 2, pp. 589–598 (2010).
11. L. Shao, A. E. HartaviKarci, D. Tavernini, A. Sornioti, M. Cheng, *Design approaches and control strategies for energy-efficient electric machines for electric vehicles-A review*, IEEE Access, **8**, pp. 116900–116913 (May 2020).
12. C. A. Bilațiu, S. I. Cosman, R. A. Marțiș, C. S. Marțiș, S. Morariu, *Identification and evaluation of electric and hybrid vehicles propulsion systems*, Proc. electric vehicles International Conf. (EV), Bucharest, Romania (03-04 Oct. 2019).
13. Z. Wang, J. Zhou, G. Rizzoni, *A review of architectures and control strategies of dual-motor coupling powertrain systems for battery electric vehicles*, Renewable and sustainable energy reviews, **162**, pp. 1–20 (July 2022).
14. S. G. Selvakumar, *Electric and hybrid vehicles – a comprehensive overview*, IEEE 2nd International Conf. on electrical power and energy systems (ICEPES), Bhopal, India, pp. 1–6 (Dec 10-11, 2021).
15. C. H. T. Lee, W. Hua, T. Long, C. Jiang, L. V. Iyer, *A critical review of emerging technologies for electric and hybrid vehicles*, IEEE Open Journal of vehicular technology, **2**, pp.471–485, (Dec. 2021).
16. G. Maggetto, J. Van Mierlo, *Electric, and electric hybrid vehicle technology: a survey*, IEEE seminar electric, hybrid, and fuel cell vehicles, Durham, UK, pp. 1–6 (April 2000).
17. M. Zeraoulia, M.E.H. Benbouzid, D. Diallo, *Electric motor drive selection issues for HEV propulsion systems: A comparative study*, Proc. of IEEE Tran. on Vehicular Technology, **55**, 6, pp. 1756–1764 (Nov. 2006).
18. T. Guilin, M. Zhiyum, Z. Libing, L. Langru, *A novel driving and control system for direct-wheel-driven electric vehicle*, IEEE Trans. on magnetic, **41**, 1, pp. 497–500 (Jan. 2005).
19. Y.P. Yang, C. P. Lo, *Current distribution control of dual directly driven wheel motors for electric vehicles*, Control engineering practice Journal, **16**, pp. 1285–1292 (2008).
20. L. Chang, *Comparison of AC drives for electric vehicles—a report on experts' opinion survey*, IEEE Aerospace and Electronic Systems Magazine, **9**, 8, pp. 7–11 (1994).
21. W. Qinglong, Changzhou, Y. Shuying, *Indirect field oriented control technology for asynchronous motor of electric vehicle*, IEEE International Conf. on power, Intelligent computing and systems, Shenyang, China, pp. 673–677 (28-30 July 2020).
22. X. Xiao-Feng, L. Guo-Feng, H. Rong-Tai, *Rotor field-oriented vector control system for electric traction application*, Proc. of the IEEE International symposium on industrial electronics Cholula, Puebla, Mexico, pp. 294–299, (4-8 Dec. 2000).
23. S. M. E. Fadul, I. Aris, N. Mison; A H. Izhai, A.K.M. Parvez Iqbal, *Modelling and simulation of electric drive vehicle based on Space Vector Modulation technique and Field Oriented Control strategy*, International Conf. on Communication, Control, Computing and Electronics Engineering (ICCCCEE), Sudan (16-18 Jan. 2017).
24. A. KGR, W. Beevi M, *Indirect field-oriented control of induction motor using predictive current controller*, International Conf. on control communication & computing (ICCC), Trivandrum, India, pp. 248–253 (19-21 Nov. 2015).
25. P. BV, A. Balamurugan, T. Selvathai, R. Reginald, J. Varadhan, *Evaluation of different vector control methods for electric vehicle application*, 2nd International Conf. on power and embedded drive control (ICPEDC), Chennai, India, pp. 273–278 (21-23 Aug. 2019).
26. D. Benoudjit, N. Nait-Said, M-S, Nait-Said, *Differential Speed Control of a Propulsion System using Fractional-Order Controller*, Electromotion Journal, **14**, 2, pp. 91–98 (April-June 2007).
27. S. Yahia Chérif, D. Benoudjit, M. S. Nait-Said, N. Nait-Said, *Comparative study between propulsion system failures of an electrical vehicle piloted by FOC and by DTC using dual induction motor's structure*, Diagnostyka Journal, **21**, 3, pp. 41–47 (2020).
28. D. Benoudjit, N. Nait-Said, M-S, Nait-Said, *Robust Speed Control of a propulsion System based on Symmetrical Method*, Rev. Roum. Sci. Techn.—Électrotechn. et Énerg., **52**, 4, pp. 475–487 (2007).
29. S. Yahia Chérif, D. Benoudjit, M-S, Nait-Said, N. Nait-Said, *Incipient short circuit fault impact on service continuity of an electric vehicle propelled by dual induction motors structure*, Rev. Roum. Sci. Techn.—Électrotechn. et Énerg., **67**, 3, pp. 265–270 (2022).
30. S. Yahia Chérif, D. Benoudjit, M-S, Nait-Said, N. Nait-Said, *Wheel load torque emulation for electric propulsion structure using dual induction motors*, International Journal of Engineering, **35**, 6, pp. 1202–1222 (2022).